Cat Hemoglobin: pH-Dependent Cooperativity of Oxygen Binding

Abstract. *Cat hemoglobin has a lower cooperativity and oxygen affinity than most mammalian hemoglobins. In contrast to the usual invariance of cooperativity with* p*H, a rise in cooperativity with* p*H is predicted by the allosteric model for low-affinity hemoglobins. Such a* p*H-dependent cooperativity for cat hemoglobin has been found.*

Cat hemoglobin is unusual in that it exhibits a very low cooperativity (n = approximately 2 at pH 6.8) when compared with human and most other mammalian hemoglobins (n = 2.6 to 3.0) (*1*). In the course of comparative studies of tetramer-dimer dissociation constant ($K^{R}_{4,2}$) of various liganded mammalian hemoglobins, we discovered that cat hemoglobin also has a higher dissociation constant than other hemoglobins. Of the nine mammalian hemoglobins studied, only cat hemoglobin had a dissociation constant that differed significantly from that of human hemoglobin. The oxygen affinity and dissociation properties of cat hemoglobin suggested that it might provide an excellent system for testing the predictions of the allosteric model (*2*).

The allosteric model is based on the existence of two conformational states, R and T. The states are in equilibrium characterized by an equilibrium constant L defined (*3*) as $L = [T]/[R]$, where [T] and [R] are the concentrations in the two states. The two states possess different affinities for ligand given by the dissociation constants K_R and K_T. The significant parameter in the allosteric model is c, the ratio K_R/K_T. Additional relationships have also been derived for hemoglobin (*2*, *4*):

$$L = \frac{K^{R}_{4,2}}{K^{T}_{4,2}} = \left[\frac{P^{Hb}_{50}}{P^{ch}_{50}}\right]^{4} \qquad (1)$$

where $K^{R}_{4,2}$ and $K^{T}_{4,2}$ are the tetramer-dimer subunit dissociation constants of the liganded (R) and unliganded (T) hemoglobin states. The quantities P^{Hb}_{50} and P^{ch}_{50} represent the ligand concentrations at half saturation for hemoglobin and its chains. These relationships stem from the functional equivalence of dimers and chains (*4*, *5*). The value of P^{Hb}_{50} determines the position of a particular hemoglobin on the theoretical bell-shaped curve for dependence of cooperativity on the logarithm of L (*2*). If it is assumed that the values of P^{ch}_{50} and c for cat hemoglobin are the same as for human hemoglobin, then the P^{Hb}_{50} value places cat hemoglobin on the right side of the bell-shaped curve, predicting a value of about 2.3 for n for cat hemoglobin at pH 7. The allosteric model would then predict an increase in n with decreasing L or P^{Hb}_{50}. The alkaline Bohr effect describes the decrease in P^{Hb}_{50} with increasing pH. Cat hemoglobin has the same Bohr effect as human hemoglobin (*1*), and we have used this pH dependence of P^{Hb}_{50} to test the allosteric model. A substantial increase in the cooperativity of a mammalian hemoglobin as a function of pH has never been observed, except in the presence of inositol hexaphosphate (*6*).

Cat hemolyzates were prepared from heparinized or citrated blood samples as described by Edelstein *et al.* (*7*). The hemolyzates were stored in the oxygenated form and were discarded after 1 week. The major (A) and minor (B) cat hemoglobin components were separated on a BioRex 70 ion exchange column according to the method of Taketa and Morell (*1*), with the addition that 0.14M phosphate buffer was used to elute the A component from the column (*8*). The hemolyzates which were to be separated in this way were first flushed with carbon monoxide to prepare the carboxyhemoglobin derivative. The carbon monoxide was later removed from the purified components by photolysis immediately before use. Oxygen equilibria were attained in gas-tight tonometers fitted with 2-mm quartz cuvettes. After removal of oxygen from the sample by repeated consecutive flushing with nitrogen and evacuation, air was added from a gas-tight syringe through a rubber stopper in the tonometer, and the solution was equilibrated with gentle shaking in a water bath at 22°C for 10 or 15 minutes. Spectra between 500 and 600 mμ were recorded with a Cary 15 spectrophotometer. Five to ten points were determined for each oxygen equilibrium curve, and the results were calculated by using two different methods. In the first method we used the formulas of Benesch *et al.* (*9*), which take into consideration the concentration of methemoglobin. In the second method we neglected the presence of methemoglobin and calculated the percentage change in optical density relative to the total difference in optical density between the oxy and deoxy forms at three different wavelengths. The values of n determined by the two methods were usually in good agreement. Using the first method, we calculated the percentage of methemoglobin at each equilibrium point. When there was a significant increase in methemoglobin during the course of an experiment the results were discarded. Results from experiments containing relatively high proportions of methemoglobin (more than 15 percent) were also discarded. The points between 30 and 70 percent saturation were used in a least-squares fit of the data to determine the slope and the "log PO_2" intercept of the Hill plot. Dissociation constants were determined by both sedimentation velocity and sedimentation equilibrium methods, as described by Edelstein *et al.* (*7*). Experiments from pH 6.5 to pH 7.7 were done in 0.1M potassium phosphate, and those from pH 7.9 to pH 9 in 0.1M sodium pyrophosphate buffer. The pH of the solution was determined directly after the experiment was finished.

We determined the pH dependence of the Hill n and the P^{Hb}_{50} of cat hemoglobin. The cooperativity increases with pH (Fig. 1). Both the A and B components obtained from the ion exchange column showed more variability in cooperativity than the hemolyzate at low pH values, but they followed a similar pattern. The variability of these components is probably due to the increased instability of the isolated hemoglobins. The oxygen equilibria and ultracentrifuge results for the isolated components will be presented in a more complete report (*10*). Both components have identical values of P^{Hb}_{50} which change identically with pH; therefore, most of the experiments were performed on the hemolyzate since it is much more stable.

The pH dependence of the cooperativity of cat hemoglobin is much steeper than that expected of a simple pH titration. The data do, on the other hand, fit the curve predicted by the allosteric model very well (Fig. 2). At pH 6.5 the cooperativity of cat hemoglobin is about 2.1, and the high P^{Hb}_{50} of cat compared to human hemoglobin places this point on the lower right side of the curve. As the pH is raised P^{Hb}_{50} and thus L concomitantly decrease, and at the same time n in-

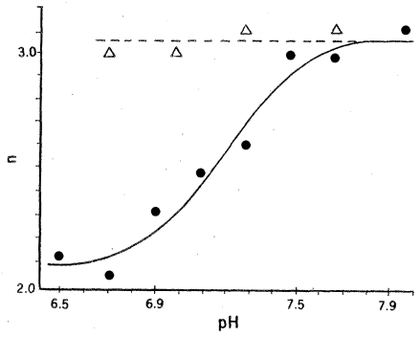

Fig. 1. The *p*H dependence of the cooperativity (n) of cat and human hemoglobins. The experiments were performed and evaluated as described in the text. (Triangles) Human hemoglobin hemolyzate (the points represent single experiments); (circles) cat hemoglobin hemolyzate (the points are averages for two to four experiments).

creases. By *p*H 8, the value of P_{50}^{Hb} for cat hemoglobin is close to the value for human hemoglobin at *p*H 7. Increasing the *p*H further does not result in a significant increase in cooperativity. Apparently the value of L now corresponds to the region of the top of the bell curve, where the cooperativity of the hemoglobin is not expected to change appreciably with *p*H. Human hemoglobin lies within this "buffered region" (*2*) throughout the *p*H range used.

In only two other cases has the cooperativity of a hemoglobin been observed to increase as a function of *p*H. The first is the case of human hemoglobin in the presence of inositol hexaphosphate, for which tabulated data have been reported (*6*). Although the authors report that the data do not fit a bell curve calculated for a value of $c = 0.008$, we find that they do fit a curve calculated for cat hemoglobin which corresponds to a value of $c = 0.0038$. This value of c is lower than that initially used to fit published data to the allosteric model (*2*). Unfortunately, no other independent measure of c for cat hemoglobin is available, but the value of c which we have chosen is well within the range of reported c's for human hemoglobin. If cat and human hemoglobins do have the same c, then a study of cat hemoglobin will provide a much more accurate estimate of the value of c than will equivalent data for human hemoglobin, since the right side of the bell curve where cat hemoglobin lies is more sensitive to the value of c.

Hemoglobin Milwaukee-1 exhibits a small *p*H-dependent cooperativity, which varies from 1.4 to 1.6 with a *p*H change from 6.5 to 7.9 (*11*). The P_{50}^{Hb} of hemoglobin Milwaukee-1 is about 13 mm-Hg at *p*H 7 compared to 26 mm-Hg for cat hemoglobin at *p*H 7. Since hemoglobin Milwaukee-1 contains only two functional heme groups it cannot be placed on the same bell curve as a tetramerically functional hemoglobin. The maximum of the bell curve for n plotted against log L occurs at $L = c^{-i/2}$, where i is the number of functional heme groups (*12*). Thus, the maximum of the curve for a dimerically functional hemoglobin would be far to the left of that for a tetramerically functional molecule (Fig. 2). This would place hemoglobin Milwaukee-1 on the lower right side of its respective curve, and the allosteric model would predict that this molecule should have both a lower cooperativity and a smaller increase in cooperativity with *p*H than does cat hemoglobin. The data presented by Hayashi *et al.* (*11*) roughly follow the predicted bell-shaped curve with $c = 0.0038$, but as the data were presented in the form of a graph and the values for specific points were not tabulated only a crude estimate of the fit could be made.

For several human hemoglobin derivatives (*13*) cooperativity has been found to decrease with *p*H. These are all high-affinity forms, and should be on the left side of the bell curve. The decrease in cooperativity with *p*H is generally compatible with the allosteric model, but some of the modifications involved may modify the heme environment, which could alter c, leading to a different bell curve.

In addition to a dramatic *p*H dependence of cooperativity, the allosteric model predicts a change in the ratio of the subunit dissociation constants ($K_{4,2}^{R}$ and $K_{4,2}^{T}$) of the R and T forms as a function of *p*H (Eq. 1). We have found that $K_{4,2}^{R}$ of cat hemoglobin decreases from about 30 μM at *p*H 7 to about 9 μM at *p*H 8. The $K_{4,2}^{R}$ for human hemoglobin at *p*H 7 is $2 \times 10^{-6} M$. Thus. it appears that the main source of the difference in L for human and cat hemoglobins at *p*H 7 is the order of magnitude higher dissociation constant for liganded cat hemoglobin.

The results presented here are in close agreement with the predictions of the allosteric model. It remains to be seen if cat hemoglobin has the same value of c as human hemoglobin and if the other hemoglobins mentioned here can also be treated with the same value of c. Independent estimates of c from kinetic measurements (*14*) or extensive oxygen equilibria (*15*) would be of value. As emphasized by Bunn and Guidotti (*6*) such estimates are especially important for hemoglobin varients where large changes in c may occur. In addition (*10*), cat hemoglobin can be prepared in a form that does not fit a single bell curve, which indicates that c may be changing slightly with *p*H. Therefore, what can be concluded from these and related studies is that c is not necessarily fixed for hemoglobins under all conditions. Rather, the existence of some sets of data that fit the allosteric model with constant c suggests the validity of the general formulation of an allosteric equilibrium between states.

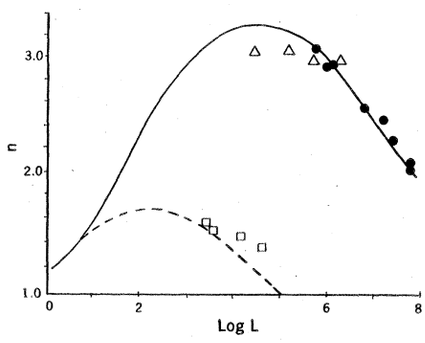

Fig. 2. Dependence of cooperativity (n) on log L. The solid line represents the theoretical curve, where n was taken to be the average slope of the Hill plot over the range of 30 to 70 percent oxygen saturation. The dashed line gives the curve for hemoglobin with only two of the four hemes capable of binding ligand. (Triangles) Human hemoglobin hemolyzate; (squares) human hemoglobin Milwaukee-1; (circles) cat hemoglobin hemolyzate. The values $c = 0.0038$ and $P_{50}^{ch} = 0.38$ were used to calculate the theoretical curve for cat and human hemoglobins, and $c = 0.0038$ and $P_{50}^{ch} = 0.29$ were used for hemoglobin Milwaukee-1. The value of $P_{50}^{ch} = 0.38$ is an average for isolated α and β chains, while the value $P_{50}^{ch} = 0.29$ corresponds to isolated α chains, since only α chains are functional in hemoglobin Milwaukee.

MARIT N. HAMILTON
STUART J. EDELSTEIN
Section of Biochemistry and Molecular Biology, Cornell University, Ithaca, New York 14850

References and Notes

1. F. Taketa and S. A. Morell, *Biochem. Biophys. Res. Commun.* **24**, 705 (1966).
2. S. J. Edelstein, *Nature* **230**, 224 (1971).
3. J. Monod, J. Wyman, J.-P. Changeux, *J. Mol. Biol.* **12**, 88 (1965).
4. J. Thomas and S. J. Edelstein, *J. Biol. Chem.*, in press.
5. S. J. Edelstein and Q. H. Gibson, in *Probes of Structure and Function of Macromolecules and Membranes*, B. Chance, T. Yonetani, A. S. Mildvan, Eds. (Academic Press, New York, 1971), vol. 2, p. 417; M. E. Anderson, J. K. Moffat, Q. H. Gibson, *J. Biol. Chem.* **246**, 2796 (1971).

6. H. E. Bunn and G. Guidotti, *J. Biol. Chem.* **247**, 2345 (1972).
7. S. J. Edelstein, M. J. Rehmar, J. S. Olson, Q. H. Gibson, *ibid.* **245**, 4372 (1970).
8. F. Taketa, A. G. Mauk, J. L. Lessard, *ibid.* **246**, 4471 (1971).
9. R. Benesch, G. Macduff, R. E. Benesch, *Anal. Biochem.* **11**, 81 (1965).
10. M. N. Hamilton and S. J. Edelstein, in preparation.
11. A. Hayashi, T. Suzuki, K. Imai, H. Morimoto, H. Watari, *Biochim. Biophys. Acta* **194**, 6 (1969).
12. M. M. Rubin and J.-P. Changeux, *J. Mol. Biol.* **21**, 265 (1966).
13. J. B. Kilmartin and J. A. Hewitt, *Cold Spring Harbor Symp. Quant. Biol.* **36**, 311 (1971).
14. Q. H. Gibson, *J. Biol. Chem.* **245**, 3285 (1970).
15. I. Tyuma, K. Omari, K. Shimizu, *Biochem. Biophys. Res. Commun.* **44**, 682 (1971).
16. Supported by grants from the National Science Foundation (GB-8773) and National Institutes of Health (HL 13591-02).

27 July 1972

Visual Receptive Fields Sensitive to Absolute and Relative Motion during Tracking

Abstract. *Some neurons in the visual cortex of awake monkeys visually tracking a moving target showed receptive fields that were excited only by stimulus motion relative to a background, while other neurons responded to any kind of stimulus motion. This result was found with two methods, one in which tracking eye movements were identical in both relative-motion and absolute-motion conditions, and another in which stimulus motions on the retina were identical in both conditions. This response pattern can differentiate translation of the retinal image during eye movement from motion of objects in the world.*

Image motion across the retina does not necessarily provide information about object motion in the world; information about object motion is generated only when one pattern in the optic array moves with respect to another. To detect motion of objects in the world, some cells in the visual system must respond to motion relative to a background (which indicates object motion) rather than to displacement of the entire visual image across the retina (which indicates eye movement). The two conditions were separated by exploring the visual receptive fields (RF's) of single cells in the monkey's visual cortex (*1*, *2*) while the monkey tracked a slowly moving target. In one condition a stimulus was fixed to a screen so that its image scanned the retina during the monkey's slow eye movement; the stimulus moved with respect to the retina but not with respect to the background. In the other condition the stimulus moved with respect to both the retina and the background during identical slow eye movements.

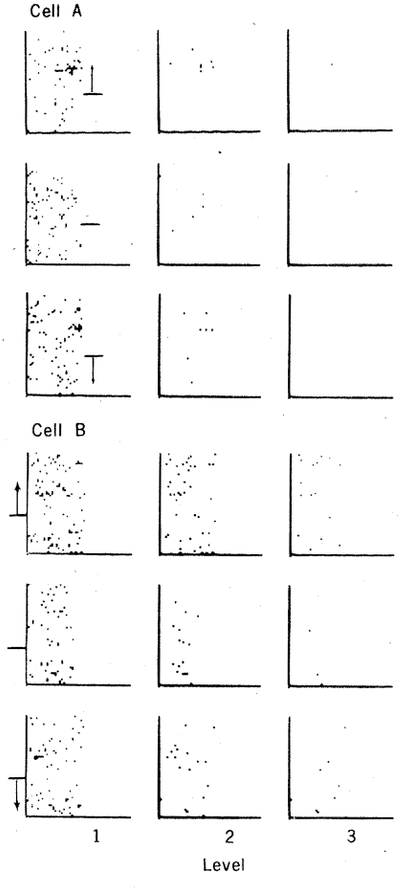

Fig. 1. Two cells with receptive fields responsive only to motion relative to a background. Each row shows a separate map made under visual tracking, and each pair of axes represents the 25° by 25° region of the stimulus screen over which the fixation target could be moved. A map consists of vertical scans separated by 0.5°, beginning at the left. Each scan is divided into 50 segments, each 0.5° (50 msec) long, and a spot is darkened in the display if the cell fired while the fixation target (a 1° disk) crossed the corresponding region of visual space. At levels 2 and 3 a spot is darkened only if the cell fired at least two or three times, respectively. The bar stimuli and their locations in relation to the scanned area are shown in the left column, with the stimuli moving through a 2° by 4° aperture in the directions indicated by the arrows attached to them. Moving bars are depicted in the centers of their apertures. About half of the 25° by 25° stimulus space was mapped in each condition. Receptive fields are apparent when the stimuli are moving but not when they are fixed on the screen. The two cells are from opposite hemispheres of the same monkey. Cell A shows one of the strongest fields found, and cell B one of the weakest. Control maps, with the fixation target moving upward but not tracked, showed only background activity (not illustrated).

Three immature rhesus monkeys were trained to sit in a primate chair and optically track a 1° target moving on a tangent screen. Eye movements were monitored with standard clinical electrooculogram electrodes fixed above and below the orbits, while the eyes were observed with a system based on the Mackworth eye camera (*3*). Because tracking accuracy improves with practice (*4*), each monkey was overtrained for at least 2000 trials before RF exploration began.

For RF determination a 25° by 25° region of the screen was divided conceptually into 2500 blocks, each 0.5° by 0.5° in extent. The fixation target passed through each block in succession, and a point was produced in the display when an action potential occurred. The displays of Fig. 1 are therefore maps of cell firing for corresponding positions of the fixation target on the screen. The target jumped to the edge of the scanned area, moved up and down (or right and left) at 10° sec^{-1}, and jumped back to a hidden origin point. If the monkey followed the downward movement of the target without saccadic eye movements, he was rewarded with apple juice. At any time the experimenter could initiate a new trial 0.5° to the right of the previous one; unsuccessful trials were repeated.

Each RF map was made with two stimuli on the screen, a fixation target and a mapping stimulus. To provide a mapping stimulus that moved relative to the screen, a horizontal bar 0.5° high was moved vertically through a fixed aperture 2° high and 4° wide. As the bar disappeared from one edge of the aperture it was replaced by another on the opposite edge, resulting in a moving display with a contant speed and direction. Light flux at the monkey's eye varied less than 1 percent as one bar replaced another. The aperture was always mounted contralateral to the hemisphere in which the cells investigated were located. With this apparatus, responses were mapped under three conditions of stimulus motion; the bars moved down the screen at 5° sec^{-1}, remained fixed, or moved up at 5° sec^{-1}. When the monkey's eye